Migas *et al. Nano Convergence* (2015) 2:16
DOI 10.1186/s40580-015-0044-8

Nano Convergence
a SpringerOpen Journal

RESEARCH Open Access

Revising morphology of ⟨111⟩-oriented silicon and germanium nanowires

Dmitri B Migas[1*], Victor E Borisenko[1], Rusli[2] and Cesare Soci[3]

Abstract

By means of *ab initio* calculations we show that morphology of ⟨111⟩-oriented silicon and germanium nanowires is defined by {112} and {011} facets. Changes in nanowire morphology are predicted to involve a partial transformation of {011} facets in favor of {112} facets even though the latter ones act as edges between adjacent {011} facets. Our estimates of surface energies clearly indicate a (112) surface to be thermodynamically preferable with respect to a (011) surface for both silicon and germanium. These findings can explain experimental observations of {112} facets in round-like and triangle-like morphologies of ⟨111⟩-oriented silicon nanowires.

Keywords: Nanowire; Morphology; Stability

1 Background

Nowadays silicon and germanium nanowires (SiNWs and GeNWs) are considered to be promising and, at the same time, accessible building blocks for various applications at nanoscale [1]. In fact, SiNWs and GeNWs having mostly ⟨011⟩, ⟨111⟩ and ⟨112⟩ orientations can easily be grown by different methods involving the vapor-liquid-solid growth mechanism [1-3]. Experimental data also indicate a clear faceting nature of morphology of these nanostructures [3,4] while theoretical calculations of the total energy of SiNWs show morphology, which is characterized by various facets, to be one of the key parameters to define the growth orientation especially at small diameters of the NWs when the surface energy is comparable to or dominates over the volume energy [5].

It is also widely accepted that the Wulff construction can predict morphology of a NW on the basis of precise information on surface energies of different surfaces. In the case of silicon the most thermodynamically stable surfaces according to experimental observations are (111), (001), (113) and (011) [6], that is also supported by results of *ab initio* calculations [7,8]. For germanium one can expect the same issue because of the same nature of chemical bonding in silicon and germanium and of comparable differences in surface energies for various surfaces with respect to silicon as theoretically predicted [7,8]. In addition to these low index surfaces, some other surfaces such as Ge(105) with the relatively low surface energy [9] should also be taken into account. This surface in the case of the proper surface reconstruction is found to be thermodynamically stable and it appears on facets of germanium pyramids formed during heteroepitaxial growth of Ge on Si(001) [10]. Thus, morphology of ⟨111⟩-oriented SiNWs and GeNWs as suggested by the Wulff construction could be characterized by {011} facets. It is also possible to use {112} facets which play the role of edges between adjacent {011} facets in order to avoid an appearance of surface atoms with two dangling bonds [5]. However, there is some experimental evidence that mainly {112} facets define morphology of SiNWs with ⟨111⟩ axes and with diameters in the range of 50 – 100 nm [11-16]. The latter fact obviously contradicts the common assumption that the Si(112) and Ge(112) surfaces are less stable (or unstable at all) than any of the (111), (001), (113) and (011) ones. There is one paper [17] where Si(112) surface with the 1×1 and 2×1 reconstructions has been investigated by first principles techniques indicating the rebonded 1×1 reconstruction to be thermodynamically stable even though the difference in surface energy between these two surface reconstructions was marginal. In addition, Si(112) surface was shown to be quite competitive in surface energy with respect to (100) and (111) ones. However, the slab thickness in these calculations was about 0.5 nm and

*Correspondence: migas@bsuir.by
[1] Belarusian State University of Informatics and Radioelectronics, 6 P.Browka, 220013 Minsk, Belarus
Full list of author information is available at the end of the article

Springer

© 2015 Migas et al.; licensee Springer. This is an Open Access article distributed under the terms of the Creative Commons Attribution License (http://creativecommons.org/licenses/by/4.0), which permits unrestricted use, distribution, and reproduction in any medium, provided the original work is properly credited.

an interaction between opposite surfaces in such a slab could not be excluded. The latter fact can affect values of calculated surface energy. Moreover, another estimates of surface energies for the Si(112) and Ge(112) surfaces with respect to the other surfaces have been done by the modified embedded atom method [18]. However, in such calculations neither structural optimization nor surface reconstruction has been performed [18]. Thus, the predicted relative stability of Si(112) and Ge(112) in Refs. 17 and 18 remains questionable and the appearance of the {112} facets in morphology of SiNWs is not fully understood.

In this paper we present results demonstrating stability of ⟨111⟩-oriented SiNWs and GeNWs with different morphology obtained by means of the total energy projector-augmented wave method and provide theoretical evidence that {112} facets are really thermodynamically stable and can define the shape of these nanostructures.

2 Methods

The structural optimization of SiNWs and GeNWs has been performed by utilizing the first principles total energy projector-augmented wave method (code VASP) described in detail elsewhere [19-21]. Exchange and correlation potentials were included using the generalized gradient approximation of Perdew-Burke-Ernzerhof [22] in the case of SiNWs and the local density approximation of Ceperly and Alder by the parameterization of Perdew and Zunger [23] for GeNWs. We have applied both the generalized gradient approximation and the local density approximation because the former describes better ground state properties for silicon while the latter fits better germanium. Since no direct comparison between values calculated for silicon and germanium surfaces and/or NWs is planned, our choice of the two approximations looks reasonable. We have considered ⟨111⟩-oriented SiNWs and GeNWs with different cross sections and diameters, while periodic boundary conditions have been applied along the NW axis with the unit cell parameter ($a_{\parallel}$). In order to provide a negligible interaction between neighboring NWs at least 7 Å of vacuum were introduced. The futher increasing in the vacuum thickness did not noticeably affect the total energy. All atoms in SiNWs and GeNWs were allowed to relax. We set the energy cutoff at 300 eV for SiNWs and at 225 eV for GeNWs. The grid of $1\times1\times6$ Monkhorst-Park points was used in calculations. Atomic relaxation was stopped when forces on the atoms were smaller than 0.04 eV/Å. To assure the convergence, the final iterations have been performed on the $1\times1\times10$ grid. The optimization of $a_{\parallel}$ was done by gradually increasing/decreasing its value along with the relaxation of the atomic positions till the equilibrium was reached. The bulk lattice parameters (a_{Si} and a_{Ge}) were found to be 5.467 Å and 5.646 Å, respectively. The initial $a_{\parallel}$ was set at $\sqrt{3}a_{Si}$ for SiNWs or at $\sqrt{3}a_{Ge}$ for GeNWs.

In order to calculate surface energies of the (112), (011), (001) and (111) silicon and germanium surfaces we have considered periodic arrangement of slabs separated by 7 Å of vacuum as in the case of NWs. Each slab had thickness of about 4 nm and it was characterized by two equal surfaces. Such a thickness was enough to assure convergence in surface energy with respect to the slab thickness. All of the atoms in the slab were allowed to relax. We adopted the same exchange and correlation potentials and energy cut-off as for SiNWs and GeNWs. The convergence in surface energy was found to be satisfactory (less than 0.01 eV/Å^2) on the grid of $9\times9\times1$ Monkhorst-Pack points for the (112), (011) and (001) surfaces and on the grid of $7\times15\times1$ Monkhorst-Pack points for the (111) surfaces. Atomic relaxation was stopped when the forces on atoms were less than 0.01eV/Å. The surface energy is calculated as a difference between the energy of a silicon or germanium atom in the bulk multiplied by the number of atoms in a slab and the total energy of a slab. Then this difference can be expressed per unit cell or square unit area. In order to calculate a dependence of the surface energy on an in-plane lattice parameter, we have eliminated any residual elastic effect caused by compression or expansion of an in-plane lattice parameter for corresponding bulk cases, where the tetragonal-like distortion has occurred in the unit cell to construct a slab along with relaxation of the lattice parameter which is perpendicular to the corresponding surface plane. This approach has been successfully applied to Ge(105) [9].

3 Results and discussion

3.1 Morphology of SiNWs and GeNWs

According to the Wulff construction morphology of SiNWs and GeNWs in the ⟨111⟩ orientations can be described by {011} and {112} facets where the latter ones are relatively small in size and act as edges between adjacent {011} facets to avoid appearing of surface atoms with two dangling bonds [5]. Surface reconstruction on the {112} facets involves formation of pentagon-like structures with dimerization of atoms with two dangling bonds [5] leading to the 2×1 reconstruction and being very similar to the reconstructed Si(113) and Ge(113) surfaces [8]. Corresponding cross sections in the case of SiNWs are shown in Figure 1. It is evident that after structural optimization the shape of NWs is rounded and faceting is “virtually” eliminated. In fact, this behavior is particularly pronounced for SiNWs with diameters of 1.5 and 2.5 nm (Figure 1, the bottom panel). Another interesting feature is a transformation of a portion of the {011} facets in favor of the {112} ones. The same issue has been observed for the ⟨011⟩- and ⟨112⟩-oriented SiNWs where

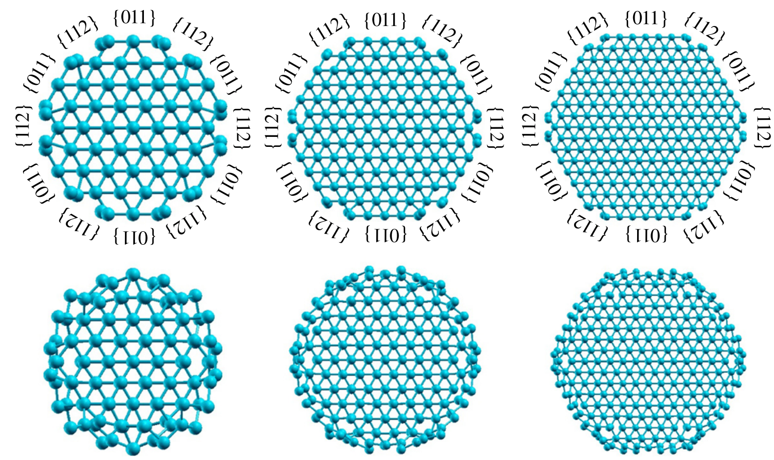

Figure 1 Cross sections of ⟨111⟩-oriented SiNWs with morphology determined by the {011} facets. All facets are indicated. The top panel: as cut from the bulk with some surface atoms having two dangling bonds on the {112} facets to be shifted towards each other in order to form dimers. The bottom panel: after structural optimization. The diameters of the SiNWs are 1.5, 2.5 and 3.4 nm (from left to right).

the {011} facets were transformed into the {111} and {113} facets, respectively [5].

We have also constructed ⟨111⟩-oriented SiNWs and GeNWs with the {011} facets playing the role of edges. Thus, the {112} facets characterize the shape of these nanostructures as shown in Figure 2 in the case of SiNWs. Similar morphology has been observed in experimentally grown SiNWs [12,15,16]. After structural optimization faceting is preserved while the {011} facets are mostly converted to the {112} ones except for the NW with diameter of 1.9 nm. Since the smallest {112} facet with the 2×1 reconstruction, which is not acting as an edge, can only appear on NWs with diameters of 2.7 nm or larger, SiNWs and GeNWs with diameters of about 2 nm possess non-reconstructed {112} facets. In fact, there are three surface atoms with two dangling bonds, where the two of these atoms at the edges also belong to the {011} facets, and that is obviously not enough to form two dimers. Instead, the atom in the middle of each {112} facet with two dangling bonds is found to be overcoordinated because two atoms at edges are shifted toward it. Another experimentally observed morphology of SiNWs displays alternate small and large in size {112} facets bounded in the triangle-like shape [11-16] as presented in Figure 3. We have also introduced here the {011} facets between the adjacent {112} facets with the 2×1 reconstruction which act as edges in order to avoid appearing of surface atoms with two dangling bonds. As in the cases described above the {011} facets are mostly transformed into the {112} ones after structural optimization. To this

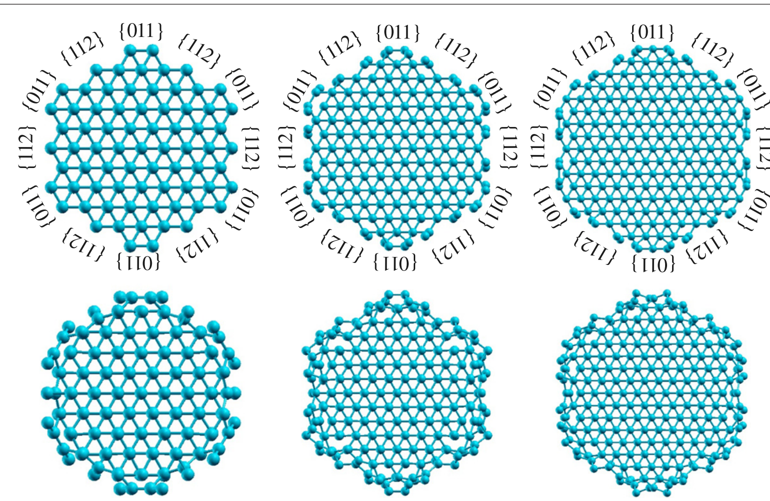

Figure 2 Cross sections of ⟨111⟩-oriented SiNWs with morphology determined by the {112} facets. All facets are indicated. The top panel: as cut from the bulk with some surface atoms having two dangling bonds on the {112} facets to be shifted towards each other in order to form dimers. The bottom panel: after structural optimization. The diameters of the SiNWs are 1.9, 2.7 and 3.1 nm (from left to right).

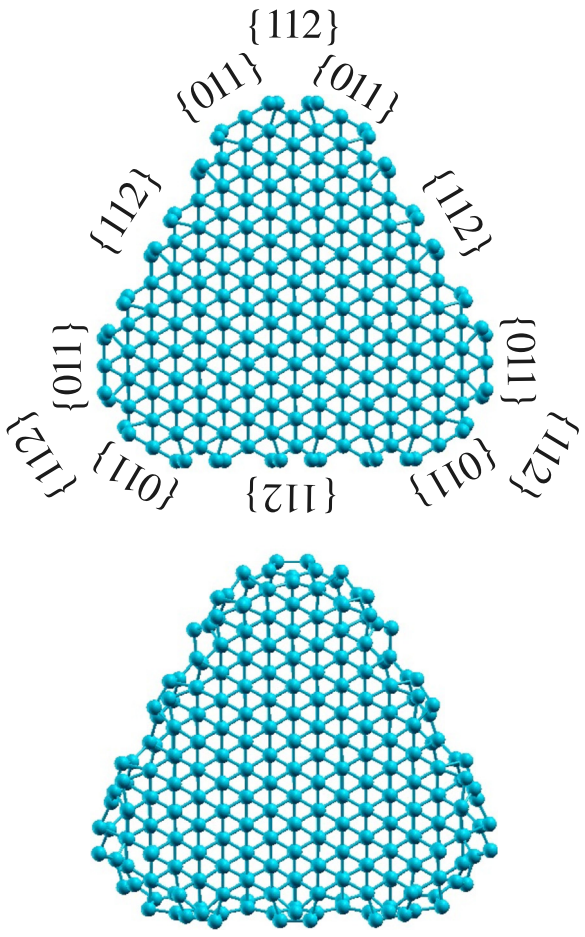

Figure 3 Cross sections of ⟨111⟩-oriented SiNWs with morphology determined by the {112} facets and bounded in the triangle-like shape. All facets are indicated. The top panel: as cut from the bulk with some surface atoms having two dangling bonds on the {112} facets to be shifted towards each other in order to form dimers. The bottom panel: after structural optimization. The diameter of the SiNW is 3.1 nm.

end, we have also checked structures of NWs, where the rebonded 1×1 reconstruction of {112} facets is involved, which have always shown some atoms with two dangling bonds located at edges.

GeNWs after relaxation are characterized by almost the same features as we have already described for SiNWs. One noticeable difference can be easily spotted by analyzing the lattice parameter along the wire axis ($a_{\|}$) which is summarized in Table 1. It is evident that SiNWs possess $a_{\|}$ to be slightly larger than the bulk lattice parameter independently of morphology. The largest expansion of $a_{\|}$ is about 1 % for the SiNW with the diameter of 1.5 nm (Figure 1, the left panel). There is only one exception for the SiNW with the diameter 1.9 nm and nonreconstructed {112} facets (Figure 2, the left panel) where $a_{\|}$ is reduced by 0.6 %. However, in the case of GeNWs a reduction of $a_{\|}$ is typical. For example, the maximal deviation of 3.8 % is detected for GeNWs with the diameter of 1.6 nm (Figure 1, the left panel) whereas 6.3 % are found for the nanostructure with the diameter of 2.0 nm and nonreconstructed {112} facets (Figure 2, the left panel).

3.2 Stability of SiNWs and GeNWs

Figure 4 presents the dependence of the total energy per atom on the number of atoms in a unit cell for SiNWs and GeNWs with different morphologies. Strictly speaking SiNWs with reconstructed {112} facets (Figure 2) have turned out to be thermodynamically preferable if their diameter is about 2.7 nm and larger (Figure 4, the top panel). At smaller diameters, when reconstruction of the {112} facets is not possible, SiNWs can be characterized by the {011} facets (Figure 1). However, the difference in the total energy for SiNWs with different morphologies and diameters larger than 3 nm is not significant and it is hard to unambiguously state that morphology with {112} facets (Figure 2) is the most stable. Surprisingly enough, SiNWs in the triangle-like shape (Figure 3) according to our data can be also quite thermodynamically competitive and appear during growth even for nanostructures with smaller diameters than experimentally observed (about 100 nm) [11-16]. Since our calculations have been performed at zero temperature, the entropic contribution to the total energy was neglected. For the ⟨100⟩-oriented SiNWs with different morphologies energy differences at finite and zero temperatures are estimated to be negligible [24]. In the case of SiNWs with ⟨111⟩ orientations experimental observations have clearly indicated {112} facets to dominate [11-16] pointing out that the entropic contribution could even promote the appearance of latter facets. It should be noted here that the results obtained in this study do not alter the order of curves representing stability of SiNWs with ⟨001⟩, ⟨011⟩, ⟨111⟩ and ⟨112⟩ axes via the dependence of the total energy with respect to the number of atoms in the unit cell as indicated in Figure seven of Ref. 5.

In general, the corresponding dependencies for GeNWs (Figure 4, the bottom panel) are similar to the ones of SiNWs. Nevertheless, GeNWs with the nonreconstructed {112} facets are predicted to be thermodynamically competitive. This issue can stem from the fact that such a GeNW is characterized by $a_{\|}$, which deviates by 6.3 % from the bulk value, providing in turn a significant lowering of the surface energy even at the expense of the bulk energy. In addition, the triangle-like morphology (Figure 3) is not expected for GeNWs having small diameters. This morphology can appear at larger diameters of a NW, when the volume energy dominates over the surface energy, and/or it is mainly defined by the interface energy between a catalytic particle and a NW.

Table 1 The diameter (*d*, nm), the number of atoms in the unit cell (*N*) and the lattice parameter along the wire axis ($a_{\|}$, Å) for SiNWs and GeNWs with different morphologies after structural optimization

	Si{011}					Si{112}			Si{112}-t
d	1.5	2.1	2.5	3.0	3.4	1.9	2.7	3.1	3.1
N	110	170	242	326	422	146	266	362	338
$a_{\|}$	5.524	5.483	5.473	5.470	5.469	5.432	5.486	5.470	5.480
	Ge{011}					Ge{112}			Ge{112}-t
d	1.6	2.2	2.6	3.1	3.5	2.0	2.8	3.2	3.2
N	110	170	242	326	422	146	266	362	338
$a_{\|}$	5.429	5.513	5.562	5.588	5.607	5.292	5.552	5.581	5.579

For the simplicity reason Si{011} and Ge{011} denote morphology of SiNWs and GeNWs shown in Figure 1, whereas Si{112}, Ge{112} correspond to the cases in Figure 2 and Si{112}-t, Ge{112}-t indicate morphology presented in Figure 3. The lattice parameters of bulk silicon and germanium are $a_{Si} = 5.467$ Å and $a_{Ge} = 5.646$ Å. $a_{\|}$ is rescaled (divided by $\sqrt{3}$) in order to correspond to the unit of the corresponding bulk lattice parameters.

In order to understand the thermodynamic background of the appearance of the {112} facets in morphology of grown SiNWs [11-16] and the reason why the transformation of the {011} facets into the {112} ones occurs in shape of SiNWs and GeNWs according to our results, we have examined the (112) surface as well as the {112} facets more in detail. The surface unit cell of the (112) surface with the 2×1 surface reconstruction is presented in Figure 5 displaying a pentagon-like structure with a dimer. This pentagon-like structure is still preserved after structural optimization for the {112} facets of SiNWs independently of morphology (Figure 5) and

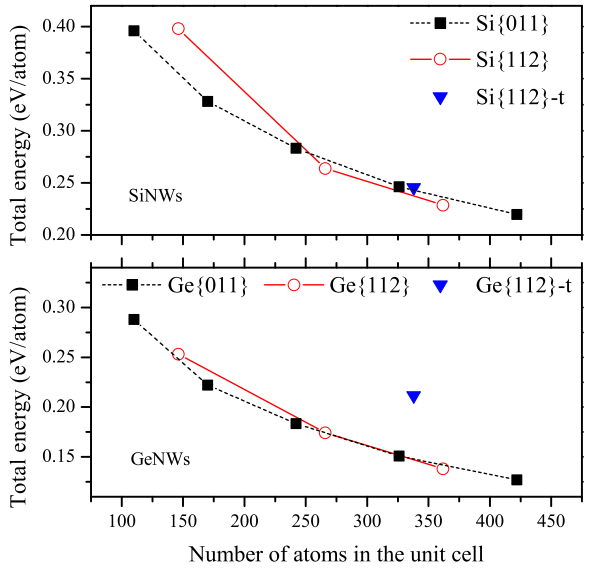

Figure 4 The total energy per atom versus the number of atoms in the unit cell for SiNWs and GeNWs. The number of formula units is proportional to NW diameter. Zero of the energy scale corresponds to the energy of the Si or Ge atom in the bulk. The lines connecting points are a guide to the eyes. For the simplicity reason Si{011} and Ge{011} denote morphology of SiNWs and GeNWs shown in Figure 1, whereas Si{112}, Ge{112} correspond to the cases in Figure 2 and Si{112}-t, Ge{112}-t indicate morphology presented in Figure 3.

uniaxial strain of ± 2 %. The same features are also typical of GeNWs. Thus, the length of dimers is found to be 2.34 Å and 2.59 Å for silicon and germanium surfaces respectively, to be compared to 2.37 Å (the bond length in the bulk silicon) and 2.44 Å (the bond length in the bulk germanium). Moreover, this dimer length is comparable to the one for the (001) surface, namely 2.36 Å for silicon and 2.51 Å for germanium. In the case of GeNWs dimers on the {112} facets remain almost invariable (2.58–2.61 Å). On the contrary, significant changes in the dimer length on the {112} facets are revealed for SiNWs with different morphologies: 2.28–2.49 Å. Dimer tilting, which is common to the (001) surface, is not detected for Si(112) and Ge(112), while distortion of the pentagon-like structure occurs for SiNWs and GeNWs. Even though the {011} facets are partly transformed into the {112} ones according to cross section views (Figures 1– 3), first neighbors of surface atoms are almost the same indicating no crucial atom reshuffle on the surface. It should be pointed out here that the size of the unit cell of Si(112) and Ge(112) shown in Figure 5 is larger than than the size of the corresponding {112} facets of SiNWs and GeNWs presented in Figure 1.

Surface energies for the (011) and (112) surfaces of silicon and germanium have been calculated and summarized in Table 2. For the (011) surface the 1×1 surface reconstruction was taken into consideration. In addition, we have also performed calculations for (001) and (111) surfaces and the data obtained can serve as reference points for comparison. The $p(2\times2)$ and $p(2\times1)$ surface reconstructions are considered for the (001) and (111) surfaces, respectively. It is evident that the (112) surface with both the 1×1 and 2×1 reconstructions possesses smaller surface energies than the (011) one and, at the same time, it is slightly higher in the surface energy with respect to the (111) and (001) surfaces for both silicon and germanium. However, in the case of germanium the surface energies of the (112) and (111) surfaces are very close. In addition we could not confirm results in Ref. 17 stating that the 1×1 reconstruction was more preferable

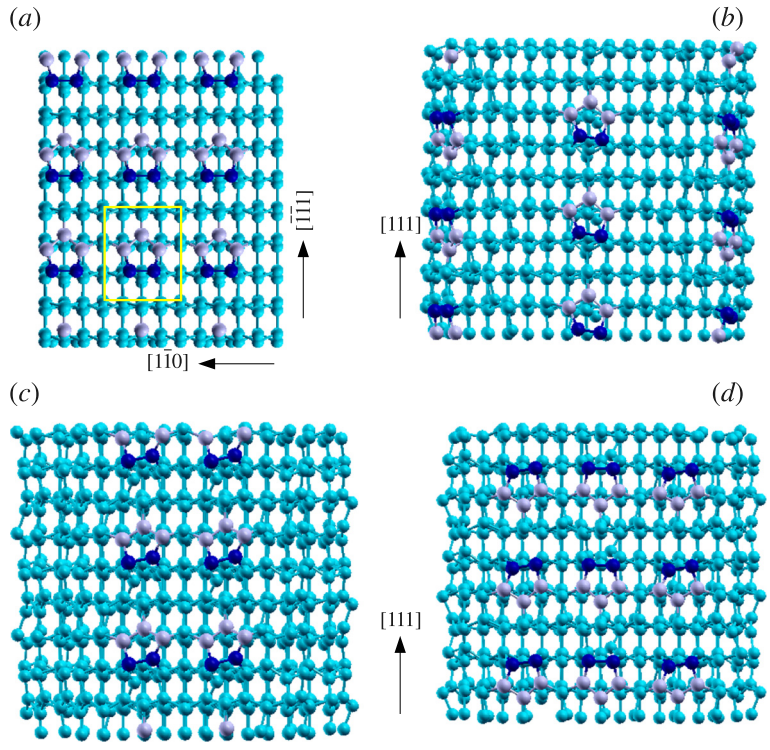

Figure 5 Views of (112) surface and {112} facets. (a) The top view of the (112) surface with the 2×1 reconstruction of silicon or germanium. The surface unit cell is indicated by the solid, yellow lines. Atoms which form the pentagon-like structure are indicated: dimer atoms are in dark blue, the rest atoms are in light gray. ***(b)*** The lateral view of the {112} facet acting as an edge in the SiNW with diameter of 3.4 nm which cross section is presented in Figure 1. **(c)** The lateral view of the large in size {112} facet in the SiNW with diameter of 3.1 nm which cross section is presented in Figure 2. ***(d)*** The lateral view of the large in size {112} facet in the SiNW with diameter of 3.1 nm which cross section is presented in Figure 3. For the lateral views ***(b)*** – ***(d)*** of SiNWs three unit cells along the wire axis are shown. Atoms involving in the the pentagon-like structures are indicated in a similar way as for the Si(112) surface ***(a)***.

in surface energy than the 2×1 one for both Si(112) and Ge(112). Thus, our results point out the 2×1 reconstruction to be more stable than the 1×1 one and justify our initial choice to use the former reconstruction on {112} facets of SiNWs and GeNWs.

We have traced how the surface energies of the (011) and (112) surfaces for both silicon and germanium change with the in-plane lattice parameter. Such dependences are shown in Figure 6. It is also convenient to present the surface energy per unit cell (Figure 6, the right panel), in our case it is the (011) surface with the 1×1 surface reconstruction, rather than per square unit area (Figure 6, the left panel) because in this case the surface energy is not directly affected by variation in square of a surface. Thus, the parabolic-like dependence of the surface energy per unit cell with respect to the in-plane lattice parameter can be observed for the selected surfaces. In the case of silicon the maximum in the surface energy of the (011) surface corresponds to the bulk lattice parameter ($\varepsilon \sim 0$ %) while for the (112) surface the maximum points to expansion ($\varepsilon \sim$ -2 %) of the in-plane lattice parameter. In the case of germanium the similar behavior is observed with the maxima in the surface energy at $\varepsilon \sim$ -1 % and $\varepsilon \sim$ -3 % for the (011) and (112) surfaces, respectively. We are aware that such calculations of the surface energy are based on an ideal surface, nevertheless we would like to project these results on facets of SiNWs and GeNWs. Thus, it is quite probable that both increasing and decreasing of $a_{\parallel}$ in SiNWs can lead to lowering in the surface energy, however such changes in $a_{\parallel}$, at the same time, does not provide lowering in the bulk energy. Only the facet nature (facets are always limited along one direction) can provide a nice opportunity to decrease the surface energy and, in turn, the total energy without valuable changing in interatomic distances of inner core atoms because of

Table 2 Surface energies (meV/Å^2) of the (112), (011), (001) and (111) surfaces of silicon and germanium

	Si	Ge
(112) with 2×1 reconstruction	89.81	72.41
(112) with 1×1 reconstruction	92.27	74.74
(011)	96.29	76.76
(001)	79.77	66.91
(111)	83.02	71.58

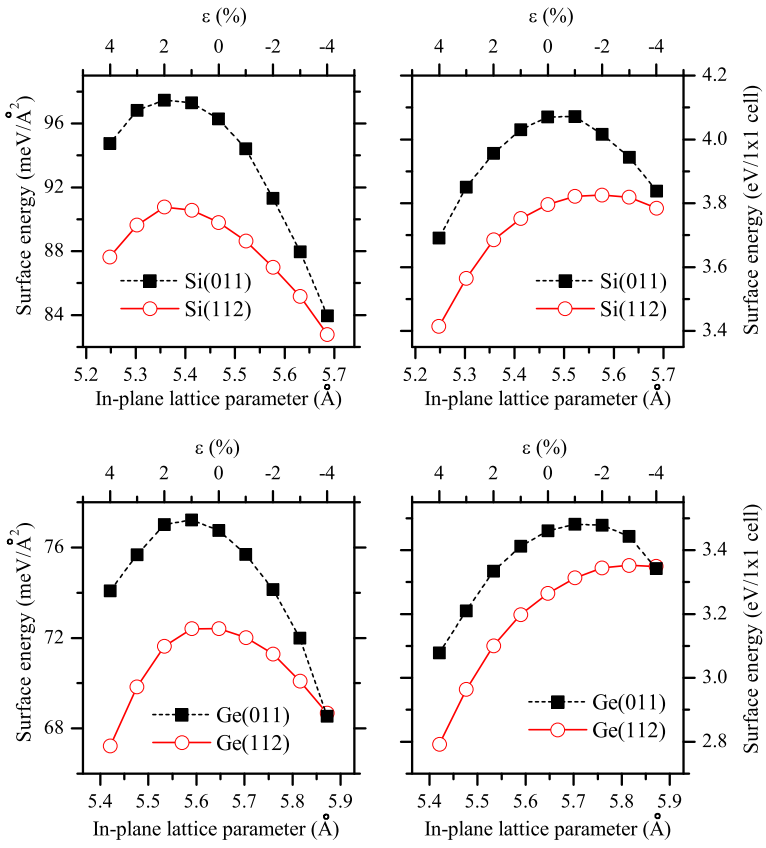

Figure 6 The surface energy of the Si(011), Si(112), Ge(011) and Ge(112) surfaces versus the in-plane lattice parameter (or strain ε).

"additional space" at edges. It is also not necessary to sizably change $a_{\parallel}$ in order to decrease the surface energy at the expense of the bulk energy. We believe this issue to be the driving force of the partial transformation of the {011} facets into the {112} ones in addition to distortion of the pentagon-like structures on the facets, which is also caused by an optimization in the *s-p* character of the surface dangling bonds. The same conclusions can be drawn for GeNWs. To this end, we expect that the (112) surface, which is similar to the (113) and (001) ones for both silicon and germanium, can preserve described features under experimental conditions during the growth process.

4 Conclusions

The results of our *ab initio* calculations confirm experimental observations that morphology of ⟨111⟩-oriented SiNWs is characterized by the {011} and {112} facets where the latter ones are predicted to define their shape if diameter of a NW is larger than 2.5 nm. The same behavior has been also observed for GeNWs. The reason of the appearance of the {112} facets in morphology of SiNWs and GeNWs is the lower surface energy of the (112) surface with respect to the (011) surface for both silicon and germanium. Thus, the common assumption that the (112) surface of silicon and germanium is unstable does not hold. Consequently, the appearance of the {112} facets which define morphology of ⟨111⟩-oriented SiNWs and GeNWs should not come as a surprise. Moreover, the triangle-like morphology with alternate large and small {112} facets of SiNWs is found to be thermodynamically competitive even for NWs with diameters starting from 3 nm. Stability of SiNWs and GeNWs in ⟨111⟩ growth directions is also improved by the transformation of a portion of the {011} facets into the {112} ones. Further lowering in the total energy can be achieved for SiNWs and GeNWs by forming the sawtooth faceting with {111} and {113} facets instead of the {112} facets as experimentally observed [11-16]. The latter is only possible for NWs with diameters starting from 100 nm because there is enough space to involve facets which are not perpendicular to the plane of the NW cross section and the triangle-like morphology is even more favorable for this purpose. Moreover, the Wulff construction is shown to be reliable to generate initial structures of SiNWs and GeNWs. Finally, our findings can be also useful in investigating of morphology of III-V NWs, such as GaAs, where many of the described features have been experimentally observed [25].

Competing interests
The authors declare that they have no competing interests.

Authors' contributions
DBM generated structural models of NWs and performed calculations. DBM, VEB and CS performed the data analysis and wrote the paper. R directed the project. All authors read and approved the final manuscript.

Acknowledgements
DBM and VEB thank the Belarusian National Research Program "Convergence" and Belarusian Republican Foundation for Fundamental Research under (Grant No. F14U-001) and Singapore Ministry of Education (project reference MOE2013-T2-1-044) for financial support. The authors are grateful to Filonov AB and Shaposhnikov VL for fruitful discussion and useful suggestions on the results of the paper. This work is supported by the Agreement on Cooperation between Belarusian State University of Informatics and Radioelectronics and Nanyang Technological University.

Author details
[1]Belarusian State University of Informatics and Radioelectronics, 6 P.Browka, 220013 Minsk, Belarus. [2]School of Electrical and Electronic Engineering, Nanyang Technological University, 50 Nanyang Avenue, 639798 Singapore, Singapore. [3]School of Physical and Mathematical Sciences, Nanyang Technological University, 21 Nanyang Link, 637371 Singapore, Singapore.

Received: 29 December 2014 Accepted: 20 January 2015
Published online: 10 August 2015

References

1. W Lu, CM Lieber, Semiconductor nanowires. J. Phys. D: Appl. Phys. **39**, 387 (2006)
2. H Jagannathan, M Deal, Y Nishi, J Woodruff, C Chidsey, PC McIntyre, Nature of germanium nanowire heteroepitaxy on silicon substrates. J. Appl. Phys. **100**, 024318 (2006)
3. T Hanrath, BA Korgel, Crystallography and surface faceting of germanium nanowires. Small. **1**, 717 (2005)
4. Y Wu, Y Cui, CJ Barrelet, DC Bell, CM Lieber, Controlled growth and structures of molecular-scale silicon nanowires. Nano Lett. **4**, 433 (2004)
5. DB Migas, VE Borisenko, The role of morphology in stability of Si nanowires. J. Appl. Phys. **105**, 104316 (2009)
6. DJ Eaglesham, AE White, LC Feldman, N Moriya, DC Jacobson, Equilibrium shape of Si. Phys. Rev. Lett. **70**, 1643 (1993)
7. AA Stekolnikov, J Furthmüller, F Bechstedt, Absolute surface energies of group-IV semiconductors: Dependence on orientation and reconstruction. Phys. Rev. B. **65**, 115318 (2002)
8. AA Stekolnikov, J Furthmüller, F Bechstedt, Adatoms, dimers, and interstitials on group-IV(113) surfaces: First-principles studies of energetical, structural, and electronic properties. Phys. Rev. B. **67**, 195332 (2003)
9. DB Migas, S Cereda, F Montalenti, L Miglio, Electronic and elastic contributions in the enhanced stability of Ge(105) under compressive strain. Surf. Sci. **556**, 121 (2004)
10. P Raiteri, DB Migas, L Miglio, A Rastelli, H von Känel, Critical role of the surface reconstruction in the thermodynamic stability of {105}Ge pyramids on Si(001). Phys. Rev. Lett. **88**, 256103 (2002)
11. FM Ross, J Tersoff, MC Reuter, Sawtooth faceting in silicon nanowires. Phys. Rev. Lett. **95**, 146104 (2005)
12. T David, D Buttard, T Schülli, F Dallhuin, P Gentile, Structural investigation of silicon nanowires using GIXD and GISAXS: Evidence of complex saw-tooth faceting. Surf. Sci. **602**, 2675 (2008)
13. H Schmid, MT Björk, J Knoch, H Riel, W Riess, P Rice, T Topuria, Patterned epitaxial vapor-liquid-solid growth of silicon nanowires on Si(111) using silane. J. Appl. Phys. **103**, 024304 (2008)
14. T Xu, JP Nys, A Addad, OI Lebedev, A Urbieta, B Salhi, M Berthe, B Grandidier, D Stievenard, Faceted sidewalls of silicon nanowires: Au-induced structural reconstructions and electronic properties. Phys. Rev. B. **81**, 115403 (2010)
15. R Boukhicha, C Gardes, L Vincent, C Renard, V Yam, F Fossard, G Patriarche, F Jabeen, D Bouchier, Gold anchoring on si sawtooth faceted nanowires. EPL. **95**, 18004 (2011)
16. F Oehler, P Gentile, T Baron, P Ferret, M den Hertog, J Rouviere, The importance of the radial growth in the faceting of silicon nanowires. Nano Lett. **10**, 2335 (2010)
17. CH Grein, First principles calculations of Si(211) surface reconstructions. J. Cryst. Growth. **180**, 54 (1997)
18. JM Zhang, F Ma, KW Xu, XT Xin, Anisotropy analysis of the surface energy of diamond cubic crystals. Surf. Interface Anal. **35**, 805 (2003)
19. G Kresse, J Hafner, Ab initio molecular-dynamics simulation of the liquid-metal-amorphous-semiconductor transition in germanium. Phys. Rev. B. **49**, 14251 (1994)
20. G Kresse, J Furthmüller, Efficiency of ab-initio total energy calculations for metals and semiconductors using a plane-wave basis set. Comput. Mater. Sci. **6**, 15 (1996)
21. G Kresse, J Furthmüller, Self-interaction correction to density functional approximation for many electron systems. Phys. Rev. B. **54**, 11169 (1996)
22. JP Perdew, S Burke, M Ernzerhof, Generalized gradient approximation made simple. Phys. Rev. Lett. **77**, 3865 (1996)
23. J Perdew, A Zunger, Self-interaction correction to density functional approximation for many electron systems. Phys. Rev. B. **23**, 5048 (1981)
24. R Rurali, N Lorente, Metallic and semimetallic silicon ⟨100⟩ nanowires. Phys. Rev. Lett. **94**, 026805 (2005)
25. X Dai, SA Dayeh, V Veeramuthu, A Larrue, J Wang, H Su, C Soci, Tailoring the vapor-liquid-solid growth toward the self-assembly of GaAs nanowire junctions. Nano Lett. **11**, 4947 (2011)

Submit your manuscript to a SpringerOpen journal and benefit from:

- ► Convenient online submission
- ► Rigorous peer review
- ► Immediate publication on acceptance
- ► Open access: articles freely available online
- ► High visibility within the field
- ► Retaining the copyright to your article

Submit your next manuscript at ► springeropen.com